Available online at www.sciencedirect.com

SCIENCE DIRECT

Biochimica et Biophysica Acta 1664 (2004) 1–8

BIOCHIMICA ET BIOPHYSICA ACTA BBA

www.bba-direct.com

Rapid report

Applied field nonequilibrium molecular dynamics simulations of ion exit from a β-barrel model of the L-type calcium channel

Vivek Ramakrishnan[a,1], Douglas Henderson[b], David D. Busath[a,*]

[a] Department of Physiology and Developmental Biology, Brigham Young University, 574 Widstoe Building, Provo, UT 84602, USA
[b] Department of Chemistry and Biochemistry, Brigham Young University, Provo, UT, USA

Received 1 December 2003; received in revised form 15 March 2004; accepted 19 March 2004
Available online 5 May 2004

Abstract

We present results of applied field nonequilibrium molecular dynamics simulations (AF NEMD) of a minimal β-barrel model channel intended to represent an L-type calcium channel that suggests a possible relationship between glutamate side chain conformational changes and ion flux in calcium channels. The β-barrel is used to provide a scaffolding for glutamate side chains and a confinement for electrolyte of dimensions similar to the expected channel structure. It was preloaded with ions to explore relative rates of ion exit for different occupancy configurations. Our simulations with an asymmetrical flexible selectivity filter represented by four glutamate side chains (EEEE), one of which differs in initial dihedrals from the other three, indicate a plausible mechanism for the observed anomalous mole fraction effect seen in calcium channels. Apparent rates of electric field-induced exit from channels preloaded with three Na^+ ions are much higher than for channels with one Ca^{2+} followed by two Na^+ ions, consistent with the common notion that Ca^{2+} block of Na^+ current is due to competition between the Ca^{2+} and Na^+ ions for the negatively charged (EEEE) locus. In our model, the Ca^{2+} ion ligates simultaneously to the four negatively charged glutamate side chains and sterically blocks the permeation pathway. Ca^{2+}-relief of Ca^{2+}-block is suggested by a much higher rate of exit for channels preloaded with three Ca^{2+} ions than for channels with two Ca^{2+} ions.

Keywords: Calcium channel; Atomistic side chain; AF NEMD; Anomalous mole fraction effect; Selectivity filter; Glutamate conformational change

1. Introduction

Voltage-gated calcium channels play an important role in a variety of biological mechanisms in the cell and show remarkable selectivity towards Ca^{2+} ions while conducting ~ 10^6 ions per second [1]. Site-directed mutagenesis studies on the calcium channel have identified a single high affinity binding locus consisting of four glutamate residues (EEEE) in the P loop region of the α_1 subunit, which is responsible for the selectivity of the channel [1–5]. Experimental data suggest that these four glutamate side chains play an important role in ion permeation [1–7] and project into the water-filled lumen of the channel [8]. Thus, the mechanism of permeation in the Ca^{2+} channel is very different from that of the KcSA channel [9,10] in that side chains, rather than backbone carbonyls, coordinate the permeating cations. The side chains may undergo conformational changes in the process.

Open-state L-type calcium channels transport Na^+ in the absence of Ca^{2+}, are blocked by μM Ca^{2+}, and are conductive in mM Ca^{2+} solutions [11,12]. This anomalous mole fraction effect (AMFE) is commonly ascribed to Ca^{2+}-block of Na^+-current due to high binding affinity of Ca^{2+} to the EEEE selectivity filter, with relief of block at high [Ca^{2+}] by competition [11]. Although the structure of the calcium channel is still unknown, many simplified models of the selectivity filter have been evaluated for ion-binding selectivity, including phenomenological [13], ansatz [14], homogeneous colloid [15], tetra-acetate [16], β-barrel [17], infinite smooth-walled cylinder [18,19], finite smooth-walled cylinder [20–22], finite atomistic cylinder [23], finite atomistic cylinder with atomistic Glu side chains [24], and homology [25–27] models. The simpler models based on phenomenological theories and Brownian dynamics or Monte Carlo simulations have been quite successful at yielding the desired

* Corresponding author. Tel.: +1-801-422-8753; fax: +1-801-422-0700.
E-mail address: david_busath@byu.edu (D.D. Busath).
[1] Current address: Department of Physiology and Pharmacology, Oregon Health Sciences University, Portland, Oregon.

0005-2736/$ - see front matter © 2004 Elsevier B.V. All rights reserved.
doi:10.1016/j.bbamen.2004.03.015

behaviors (see especially Refs. [21,22]). But with more complete models containing explicit solvent, Ca^{2+}-block of Na^{+}-current was elusive [23] until explicit side chains were introduced [24], and Ca^{2+}-relief of Ca^{2+}-block remains difficult to simulate [24], although recent free energy studies with a homology model [26,27] are suggestively positive.

To explore this idea in more detail, we constructed a simple β-barrel channel with atomistic side chains. There is no reason to expect the P-region of a calcium channel to be a β-barrel; we have merely used this minimal motif as a flexible scaffolding on which to anchor the glutamates. The model is also minimal in that neighboring side chains, whose packing in the P-region is not yet known, are absent. The β-barrel is comprised of four individual strands of 10 glycine residues each, separated by four decapeptide strands having nine glycine residues and one glutamate residue at position 9. These eight β-strands were organized in an anti-parallel arrangement to form an eight-stranded, untilted (S = 0) β-barrel with diameter ~ 10.4 Å, because this allows room for the Glu side chains to be mobile and to simultaneously coordinate a cation. It is roughly consistent with previous estimates of the channel dimensions [15,16,20–27], after taking the finite size of the glutamate side chains into account [24]. The side chain of one of the glutamates was manually rearranged by rotations about side-chain torsions so that the Cδ was ~2.8 Å below the plane formed by the Cδs of the other three glutamate residues. This was done to represent an asymmetrical filter region, suggested by experimental studies [1,4,5]. Although the exact position of these glutamate side chains is subject to speculation [1,28], we used this simple structural arrangement as a reasonable starting point.

Molecular dynamics (MD) simulations can be performed in a canonical or an isothermal, isobaric ensemble, and can be used for nonequilibrium problems, such as steered MD simulation of atomic force microscopy [29], polymer stretching [30], and water transport through aquaporin [31] or grand canonical ensemble simulation of transport in a concentration gradient [32]. Here, we use one aspect of a similar methodology designed to simulate current flow through membrane channels when equilibrium is disturbed by application of an external electric field [33,34]. In the complete implementation, current passes continually through periodic boundaries and resistive heating is compensated with a system thermostat, producing a "steady state" on the millisecond time scale. Here, the external electric field and thermostat are used in the same way, but trajectories are truncated within a few nanoseconds after a preloaded ion escapes from Glu side chains. This method allows one to evaluate the ion-exit process, which, for channel block conditions, is probably rate-limiting. Compared to featureless channels [33,34], the glutamate side chains inhibit flow quite dramatically [24]. Therefore, we employed the statistical strategy employed in the Fold@Home protein-folding project [35]. Several different trajectories were initialized with a preloaded selectivity filter. Under the assumption that dwell times are approximately exponentially distributed, the average survival time for that preloaded state was estimated.

In this approach, the dwell time of mobile cations in the selectivity filter region was reduced to measurable lengths by the application of a strong electric field. In the spirit of steered molecular dynamics, this allowed a crude but direct measure of the differences in the barrier to ion exit for various loading states of the channel. It is reasonable to expect that the ratios of rates for different loading states, measured at high membrane potentials, would be similar to those at physiological potentials.

2. Simulation methods

2.1. System structure

The two ends and interior of the β-barrel were solvated using two spheres of TIP3P water molecules [36], each with a radius of 15 Å (a total of 620 molecules) and constrained with a spherical potential (Fig. 1A). One sphere was centered at [17.00, 0.00, 0.00] and the other at [−8.08, −0.23, −0.05]. The system was neutralized using appropriate counterions (Cl^{-} or Na^{+}, depending on the ion configuration in the filter region). For example, if the starting configuration of the selectivity filter (EEEE) had three Na^{+} ions, an extra Na^{+} ion was placed in one of the two baths such that the sum of atomic charges was equal to zero.

The channel axis was aligned with the *Z*-axis. The total number of atoms in the system was approximately 2400. A harmonic constraint was applied on the Cαs. The ions were freely mobile, but remained associated with the water, which was held within the channel sterically by the channel walls and within the water balls at each end of the channel by the spherical potential.

2.2. Force field and ensemble

All calculations were performed using the academic version c27b4 of the biomolecular simulation program, CHARMM [37]. Non-bonded cutoffs were set to a value greater than the system dimensions. During equilibration and simulation phases, an electric field of 6.67×10^{8} V/m was applied in the *Z* direction to the mobile ions in the filter region using the CHARMM PULL command, which applies a force proportional to atom charge to each selected atom. This corresponds to the field that would be experienced by an ion in a channel where a membrane potential of 2.0 V drops linearly through a distance of 30 Å. A smaller electric field, corresponding to 0.20 V of potential across a 30-Å membrane, was applied to the rest of the system. The mixed applied field was designed to simulate protein distortion and water polarization expected under reasonably realistic conditions while allowing better sampling of occupancy state transitions. The smaller applied field had minimal effects

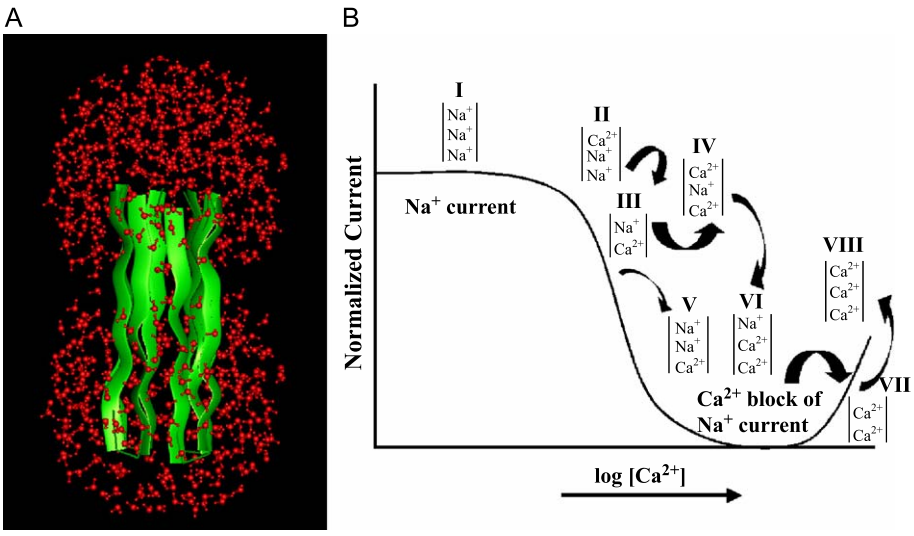

Fig. 1. (A) Side view of the eight stranded β-barrel (S = 0) structure (colored green) with two water spheres (colored red) on each end. (B) State diagrams of the various hypothetical ion configurations in the selectivity filter imposed on a stylized AMFE curve to illustrate presumed, approximate relevant loading states for the different experimental conditions. For interpretation of the references to colour in this figure legend, the reader is referred to the web version of this article.

on system configuration and temperature during the short equilibration phase and could therefore be considered representative of any physiological potential. The direction of the fields was such that cations would be driven to more negative values of z, which for convenience we will refer to as ''into the cell.'' The glutamate cluster is thus positioned at the intracellular end of the β-barrel, representing the intracellular side of the putative P-region of the calcium channel, and the water droplet at the intracellular end, which we refer to below as the intracellular droplet, conceptually represents the assumed reservoir region in the center of the membrane region [9]. The SHAKE algorithm [38] was used to constrain the lengths of bonds to hydrogen atoms.

2.3. Procedure

Ions were placed in the vicinity of the selectivity filter glutamates along the channel axis, spanning a total distance of approximately 5 Å. All runs were either terminated after 2 ns or, as far as analysis was concerned, the exit of the bottom ion. Exit was defined as the point at which the ion was no longer bound to any of the glutamate side chains (i.e. within 4 Å of a carboxylate O) and was free to move around in the bath. This point varied from one trajectory to another, but was unambiguously defined by subsequent diffusive motion and progress to the far side of the exit water droplet. In preliminary studies, a low applied voltage (0.2 V) was used for two preload configurations, $|Ca^{2+}\text{-}Na^{+}\text{-}Na^{+}|$ and $|Ca^{2+}\text{-}Ca^{2+}\text{-}Ca^{2+}|$. In five different runs of 2 ns each, only one ion exited for the total 10-ns simulation. Therefore, a 2-V applied voltage was used for the bulk of the study.

Different configurations representing probable loading states of the filter region during current flow under experimental conditions were created and multiple runs were performed on each of the loading states for better sampling (Fig. 1B). For each state, either two or three ions were positioned within ~ 5 Å of the center of the EEEE filter, which is located at $z \sim -10.5$ Å. One was placed on the channel axis at the center of the EEEE filter with $z = -10.5$ Å and, depending on the initial state of interest, either one or two cations were placed above at $z = -7.5$ Å, either on the axis (for two-ion occupancy states) or off axis by a few angstroms (for three-ion states). The positioning of the upper ion or ions was randomized and did not appear to affect the outcome because it, or they, moved considerably from their original positions long before the lower ion exited the filter. These configurations represent steps that may occur during Ca^{2+}-block of Na^{+}-current and Ca^{2+}-relief of Ca^{2+}-block in an L-type calcium channel. The arrows in Fig. 1 are intended to loosely suggest both the reaction coordinate for transport at a given concentration and the shift in the dominant reaction pathway as $[Ca^{2+}]_o$ is increased in the typical AMFE experiment.

The rationale for each case is as follows. Three Na^{+} ions were placed in the filter region to represent the experimental condition where the calcium channel is permeable only to monovalent ions (Fig. 1B, structure I). This represents the conditions expected at the extreme left end of the current vs. $\log(Ca^{2+})$ curve [4,7]. We use $|Na^{+}\text{-}Na^{+}\text{-}Na^{+}|$ as a label for this configuration. In our convention, the ion on the left will represent the topmost (i.e. positive z, or extracellular) ion in the Z-direction while the ion on the right represents the bottom (negative z, or intracellular) ion. Next, we examined the configuration $|Ca^{2+}\text{-}Na^{+}\text{-}Na^{+}|$ in the filter region (Fig. 1B, structure II). This was done to determine whether an incoming Ca^{2+} ion could cause either of two Na^{+} ions to exit from the filter. Two configurations, $|Na^{+}$-

Na^+-Ca^{2+}| and |Na^+-Ca^{2+}-Ca^{2+}| (Fig. 1B, structures V and VI), were used to evaluate Ca^{2+} block of Na^+ entry, while a slightly reorganized version of VI, |Ca^{2+}-Na^+-Ca^{2+}| (Fig. 1B, structure IV) served as a control with the same excess positive charge as structure VI. In the first case (structure V), we wished to observe whether it was possible for a single Ca^{2+} ion to coordinate all the glutamates and prevent the two Na^+ ions from entering the filter region. In the second case (VI), we explored whether two Ca^{2+} ions could prevent a single Na^+ ion from entering an electrically net neutral filter region. We also examined pure Ca^{2+} loading configurations, |Ca^{2+}-Ca^{2+}| and |Ca^{2+}-Ca^{2+}-Ca^{2+}|, to represent experimental conditions where the channel is occupied exclusively by Ca^{2+} ions (Fig. 1B, structures VII and VIII).

2.4. Molecular dynamics trajectories

The entire structure was first minimized using steepest gradient and adopted basis Newton–Raphson energy minimization algorithms [37]. A random number generator was used as a seed to assign velocities for similar starting configurations in the selectivity filter. This was followed by 0.6 ps of heating with a 1-fs time step to 300 K. Equilibration (200 ps of dynamics using a 2-fs time step) was carried out with the applied field. This was followed by multiple simulations of ~1–2 ns with the electric field applied for each preloaded state. The time step was 2 fs.

2.5. Analysis

Time-to-exit for the ion deepest in the filter was determined manually with 100-fs accuracy using plots of z_{ion} vs. t and $r_{ion\text{-}glu}$ vs. t for each trajectory. The times to exit from independent runs were assumed to be samples of a Poisson process, truncated by trajectory termination in some cases. The best estimate of the mean rate constant for exit (or its upper bound), k_{off}, was therefore taken as the number of exits observed (N) divided by the sum of all times to exit (T):

$$k_{off} = N/T \quad (1)$$

The assumption here is that an exit could take place in any short interval, δt, and that the Poisson rate constant is the probability of an exit in any one such qualified interval divided by the interval length. Because the variance of a Poisson-distributed random variable is equal to the mean, the rate constants determined from a few measurements, such as are observed here, must be taken as approximations, but qualitative trends are expected to be informative.

3. Results

A typical trajectory is illustrated in Fig. 2. This trajectory was initiated with one Na^+ ion in the filter region ($z = -10.5$ Å) and Na^+ and Ca^{2+} ions extracellular to the filter region ($z = -7.5$ Å). In Fig. 1B, this corresponds to state II. At $t = 200$ ps, the Ca^{2+} ion abruptly entered the filter region (Fig. 2B), coincident with the Na^+ ion departure from the filter. This resulted in the configuration shown in Fig. 2A, state III. The Ca^{2+} ion is well coordinated by the four Glu side chains, one of which has changed conformation so that two side chains coordinate from above and two from below. The results of all the simulations with the β-barrel model are summarized in Table 1. Due to fluctuations in the positions of the glutamate residues, the escape point varied between $z = -11$ Å and $z = -15$ Å, depending on the trajectory, but in all cases it was readily and unambiguously identified in the plot of z_{ion} vs. t. As shown in Fig. 2B, once the ion leaves the last glutamate contact, it rapidly "falls" to the bottom of the intracellular water droplet ($z \sim -18$ Å) under the force of the applied field. No reentries were observed.

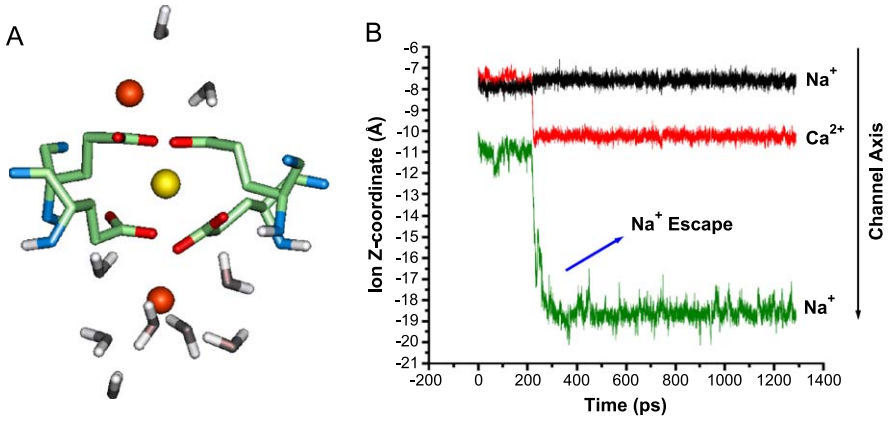

Fig. 2. (A) Configuration |Ca^{2+}-Na^+-Na^+| after 500 ps of AF NEMD simulation. The Ca^{2+} ion (yellow sphere) competes more effectively than the Na^+ ions (orange spheres) for the glutamate oxygens (colored red), thus excluding the Na^+ ions from the filter region. (B) Z-coordinate of the ions as a function of time. After expelling one Na^+ ion from the EEEE locus, the Ca^{2+} ion binds tightly to the glutamate oxygens and simultaneously prevents the binding of the second Na^+ ion to the filter region. For interpretation of the references to colour in this figure legend, the reader is referred to the web version of this article.

Table 1
Exit rates for different channel occupancies in the β-barrel model

State	Initial configuration	Number of runs	Number of escapes	Total pre-escape time (ns)	Total simulation (ns)	k_{off} (s^{-1})
I	$\|Na^+\text{-}Na^+\text{-}Na^+\|$	9	1	11.25	11.40	9×10^7
II	$\|Ca^{2+}\text{-}Na^+\text{-}Na^+\|$	5	5	1.91	6.80	2×10^9
III	$\|Na^+\text{-}Ca^{2+}\|$	4	0	8.30	8.30	$< 1.2 \times 10^8$
IV	$\|Ca^{2+}\text{-}Na^+\text{-}Ca^{2+}\|$	5	0[a]	9.00	9.00	****[b]
V	$\|Na^+\text{-}Na^+\text{-}Ca^{2+}\|$	11	0	18.20	18.20	$< 5.5 \times 10^7$
VI	$\|Na^+\text{-}Ca^{2+}\text{-}Ca^{2+}\|$	7	0	8.35	8.35	$< 1.2 \times 10^8$
VII	$\|Ca^{2+}\text{-}Ca^{2+}\|$	5	1	10.16	11.00	9×10^7
VIII	$\|Ca^{2+}\text{-}Ca^{2+}\text{-}Ca^{2+}\|$	6	6	5.60	13.20	1×10^9

Number of observed ion escapes and estimation of exit rates for various ion configurations in the selectivity filter. The applied voltage was 2.0 V for all the configurations. The k_{off} was calculated by dividing the number of escapes (for any given configuration) by the total pre-escape time (ns). A random number generator was used to initiate velocities yielding multiple distinct trajectories for each configuration.

[a] Although Ca^{2+} never exited from the filter, in every case the Na^+ ion was ejected from the filter against the applied potential.

[b] Estimate not possible, no exits observed.

From state I, $|Na^+\text{-}Na^+\text{-}Na^+|$, we observed only one escape in 11.4 ns of simulation time with nine different runs (Table 1). The estimated rate constant for escape, k_{off}, is $\sim 9.0 \times 10^7\ s^{-1}$, higher than physiologically observed exit rates ($\sim 10^6\ s^{-1}$), presumably due to the high applied potential (2 V). This value can be compared to the case with three Ca^{2+} ions, where, in each of six runs, the lower Ca^{2+} ion left the filter within 830 ps on average. The apparent exit rate constant, in this case well-defined statistically, is $1 \times 10^9\ s^{-1}$, an order of magnitude higher. Clearly the configuration $|Ca^{2+}\text{-}Ca^{2+}\text{-}Ca^{2+}|$ is less stable, probably due to the lower overall net charge in the filter region.

From state II, $|Ca^{2+}\text{-}Na^+\text{-}Na^+|$, the Ca^{2+} ion displaced a Na^+ ion in all five trajectories, the total simulation time being approximately 6.8 ns (Table 1). The calculated k_{off} is $\sim 2.0 \times 10^9\ s^{-1}$, showing that the presence of a Ca^{2+} ion increases the exit rate ~20-fold over that of the $|Na^+\text{-}Na^+\text{-}Na^+|$ state and that the Na^+ ion does not bind to the filter region very tightly. This implies that it is very probable that a single Na^+ ion or two Na^+ ions cannot prevent the Ca^{2+} ion from entering the filter region and binding to the glutamate side chains. Ion juxtaposition can be inferred by noting that the configuration in the structure (Fig. 2A) corresponds to the 500-ps point in the plot (Fig. 2B). By this point, the lower Na^+ ion has left the EEEE filter ($z = -18$ Å) and has been replaced in the center of the filter ($z = -10.5$ Å) by the middle Ca^{2+} ion. The Ca^{2+} ion is fourfold coordinated by the glutamate side chains. The upper Na^+ ion is still positioned near where it and the Ca^{2+} ion started (-8 Å $< z < -7$ Å).

State IV, $|Ca^{2+}\text{-}Na^+\text{-}Ca^{2+}|$, was unstable. All five different runs, totaling approximately 9.0 ns of simulation time, resulted in a backward ejection of the Na^+ ion against the voltage gradient such that the filter assumed the configuration $|Ca^{2+}\text{-}Ca^{2+}|$ (Table 1). This shows that an incoming Ca^{2+} ion can outcompete a Na^+ ion in binding to the negatively charged glutamate side chains while the downstream Ca^{2+} ion blocks the Na^+ exit in the forward direction.

From state V, $|Na^+\text{-}Na^+\text{-}Ca^{2+}|$, in seven different runs totaling 8.35 ns of simulation time, we observed no exits, i.e. complete Ca^{2+}-block of Na^+-exit (Table 1). Analysis of the coordinates shows that the Ca^{2+} ion is simultaneously coordinated to the four-glutamate side chains, similar to what is seen with Ca^{2+} chelators (Fig. 3), [1,3,11,39]. Similar results were observed for state III, $|Na^+\text{-}Ca^{2+}|$ where a single Ca^{2+} ion was able to prevent the entry of a Na^+ ion in the filter region. Likewise, in state VI, $|Na^+\text{-}Ca^{2+}\text{-}Ca^{2+}|$, during 18.2 ns of simulation time with 11 different trajectories, the two Ca^{2+} ions consistently prevented binding of the Na^+ ion to the glutamate side chains (Table 1). Analyses of the ion trajectories show that in all three types of simulation (starting from configuration III, V, or VI) the Ca^{2+} ions bind to the glutamate residues and prevent the entry of another Na^+ ion in the filter region (Fig. 3C and D).

From state VII, $|Ca^{2+}\text{-}Ca^{2+}|$, we observed only one escape in five different runs totaling 11.0 ns of simulation time ($k_{off} \sim 9.0 \times 10^7$, Table 1), demonstrating that the filter region binds the two Ca^{2+} ions with a moderately high affinity. The EEEE complex allows binding of the second Ca^{2+} ion despite the electrostatic repulsion from the first Ca^{2+} ion.

4. Discussion

The combination of AF NEMD simulations and the use of atomistic side chains demonstrates that a flexible selectivity filter (EEEE) is capable of demonstrating properties analogous to experimental AMFE in the calcium channel. The simulation results are consistent with the notions that: (a) Ca^{2+} ions compete successfully with Na^+ ions to bind to the glutamate oxygens, (b) Ca^{2+} ions block Na^+ current due to simultaneous binding of a single Ca^{2+} ion to the glutamate side chains, which not only occludes the permeation pathway sterically but may also, by virtue of carboxylate positioning, prevent Na^+ ions from entering the selectivity filter in spite of a net negative charge, and (c)

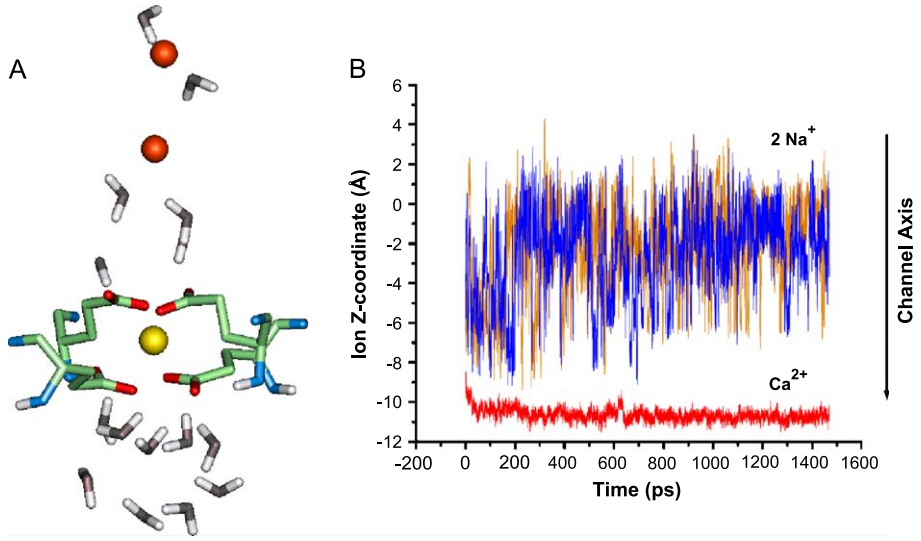

Fig. 3. (A) Configuration $|Na^{+}\text{-}Na^{+}\text{-}Ca^{2+}|$. A single Ca^{2+} ion in the filter region prevents two Na^{+} ions from entering the filter. (B) *Z*-coordinates of the two Na^{+} ions (blue and tan traces) and the Ca^{2+} ion (red trace) during an AF NEMD simulation. The Ca^{2+} ion fluctuations are small when compared to the Na^{+} ions showing that it binds to the glutamate side chains tightly, preventing the entry of Na^{+} ions. (C) Configuration $|Na^{+}\text{-}Ca^{2+}\text{-}Ca^{2+}|$. The two Ca^{2+} ions in the filter region prevent a single Na^{+} ion from entering the selectivity filter. (D) *Z* coordinates of the two Ca^{+} ions (red and purple trace) and a Na^{+} ion (blue trace). For interpretation of the references to colour in this figure legend, the reader is referred to the web version of this article.

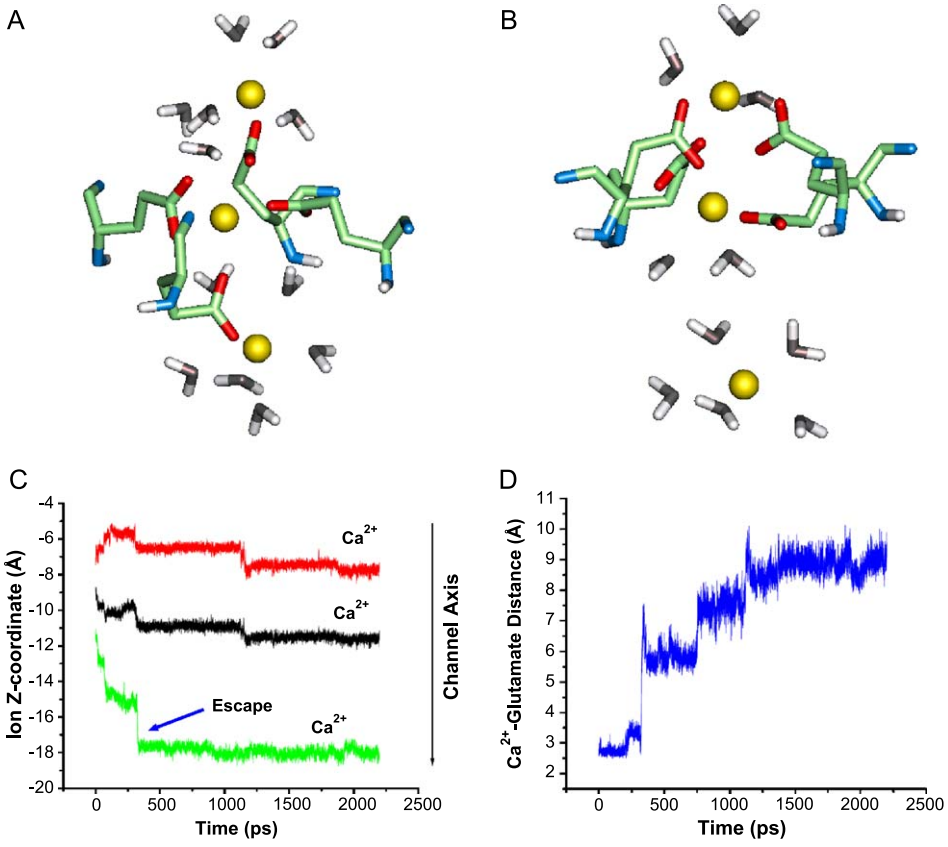

Fig. 4. (A) Configuration $|Ca^{2+}\text{-}Ca^{2+}\text{-}Ca^{2+}|$. The flexible glutamate side chains form low affinity binding sites that bind to entering and exiting Ca^{2+} ions. (B) Snapshot (450 ps) showing the exit of the Ca^{2+} ion from the filter region as the topmost Ca^{2+} ion enters the selectivity filter. (C) *Z*-coordinates of the three Ca^{2+} ions during an AF NEMD simulation. (D) Lowermost glutamate vs. exiting Ca^{2+} ion distance as a function of time.

Ca^{2+} relief of Ca^{2+} block takes place through a combination of electrostatic repulsion and stepwise changes in affinity, and may commonly involve three rather than just two Ca^{2+} ions. In this regard, the present results disagree with those of some previous calculations (e.g. Refs. [11,14,39]) that favor a maximal stable occupancy by one Ca^{2+} ion, but are consistent with other recent calculations [23,24] that suggest stable occupancy by two Ca^{2+} ions. With three Ca^{2+} ions in the filter region (state VIII), we found that the first Ca^{2+} ion is always rapidly ejected from the filter, with an apparent k_{off} rate of $\sim 1.0 \times 10^9$ (Table 1). X-ray crystal structures of several calcium binding proteins, calmodulin, calbindin, cadherin and troponin [30–43] show that it is possible that two Ca^{2+} ions can exist in close proximity. The flexible glutamate side chains could possibly provide low affinity sites that facilitate stepwise dehydration of Ca^{2+} ions.

In the presence of multiple Ca^{2+} ions, the flexible glutamate side chains in the current model were observed to undergo conformational changes that provide flanking low-affinity sites for an ion to enter and exit the selectivity filter.

In a related study [26] with a homology model based on the KcSA structure [25] having a symmetrical arrangement of filter glutamates, no Ca^{2+} ion exit was observed even from the Ca^{2+}-Ca^{2+}-Ca^{2+} preloaded state, implying that an asymmetrical selectivity filter is an important prerequisite for ion flux. Experimental studies of mutant channels lacking a single glutamate or two glutamates have shown that these channels still exhibit Ca^{2+}-block of Li^+-current [1,4,6]. This implies that tetra-coordination of the Ca^{2+} ion is not an absolute requirement for Ca^{2+} block of monovalent current and also indirectly points to the fact that the pore region is probably narrow in diameter, thus allowing a tri-coordinated or bi-coordinated Ca^{2+} ion to block the permeation pathway. Our simulations with the configuration $|Na^+$- Ca^{2+}- $Ca^{2+}|$ show that it is possible for a tri-coordinated or bi-coordinated filter to block monovalent ions from entering the selectivity filter by fully ligating the available carboxylates (Fig. 4A). Presumably a similar process might take place in the mutant channels lacking one or two glutamate residues.

Acknowledgements

We would like to thank William Sather, Steven Bogusz, Ed McCleskey, and Rick Venable for helpful comments and Christopher W. Nielsen for assistance with some of the computations. Calculations were done on SGI Origin computers of the Ira and Marylou Fulton Supercomputing Facility at Brigham Young University. This work was supported in part by NIH grant number AI23007.

References

[1] G. Varadi, M. Strobeck, S. Koch, L. Caglioti, C. Zucchi, G. Palyi, Crit. Rev. Biochem. Mol. Biol. 34 (1999) 181–214.
[2] H.R. Guy, F. Conti, Trends Neurosci. 13 (1990) 201–206.
[3] S.H. Heinemann, H. Terlau, W. Stuhmer, K. Imoto, S. Numa, Nature 356 (1992) 441–443.
[4] J. Yang, P.T. Ellinor, W.A. Sather, J.F. Zhang, R.W. Tsien, Nature 266 (1993) 158–161.
[5] M.S. Kim, T. Morii, L.X. Sun, K. Imoto, Y. Mori, FEBS Lett. 318 (1993) 145–148.
[6] P.T. Elinor, J. Yang, W.A. Sather, J.F. Zhang, R.W. Tsien, Neuron 15 (1995) 1121–1132.
[7] S.M. Cibulsky, W.A. Sather, J. Gen. Physiol. 116 (2000) 349–362.
[8] X.S. Wu, H.D. Edwards, W.A. Sather, J. Biol. Chem. 275 (2000) 31778–31785.
[9] D.A. Doyle, J.M. Cabral, R.A. Pfuetzner, A. Kuo, J.M. Gulbis, S.L. Cohen, B.T. Chait, R. MacKinnon, Science 280 (1998) 69–77.
[10] S. Berneche, B. Roux, Nature 414 (2001) 73–77.
[11] W. Almers, E.W. McCleskey, P.T. Palade, J. Physiol. 353 (1984) 565–583.
[12] I. Favre, E. Moczydlowski, L. Schild, Biophys. J. 71 (1996) 3110–3125.
[13] T.X. Dang, E.W. McCleskey, J. Gen. Physiol. 111 (1998) 185–193.
[14] C.M. Armstrong, J. Neyton, Ann. N.Y. Acad. Sci. 635 (1990) 18–25.
[15] W. Nonner, L. Catacuzzeno, B. Eisenberg, Biophys. J. 79 (2000) 1976–1992.
[16] P.S. Ganesh, B. Chanda, S.K. Gupta, M.K. Mathew, J. Chandrasekhar, Proteins 38 (2000) 384–392.
[17] S. Boguz, Molecular computations on structure and selectivity of the ß-barrel model for voltage gated potassium, sodium and calcium channel pore regions, Doctoral Dissertation, Brown University Providence, 1995 RI, 291 pp.
[18] D. Boda, D.D. Busath, D. Henderson, S. Sokołowski, J. Phys. Chem., B 104 (2000) 8903–8910.
[19] D. Boda, D. Henderson, D.D. Busath, J. Phys. Chem., B 105 (2001) 11574–11577.
[20] D. Boda, D. Henderson, D.D. Busath, Mol. Phys. 100 (2002) 2361–2368.
[21] B. Corry, T.W. Allen, S. Kuyucak, S.H. Chung, Biochim. Biophys. Acta 1509 (2000) 1–6.
[22] B. Corry, T.W. Allen, S. Kuyucak, S.H. Chung, Biophys. J. 78 (2000) 2364–2381.
[23] Y. Yang, D. Henderson, D.D. Busath, J. Chem. Phys. 118 (2003) 4213–4220.
[24] Y. Yang, D. Henderson, D.D. Busath, Molecular Simulations 30 (2004) 75–80.
[25] G.M. Lipkind, H.A. Fozzard, Biochemistry 40 (2001) 6786–6794.
[26] V. Ramakrishnan, Molecular computations on selectivity and permeation in ion channels and transporters, Doctoral Dissertation, Brigham Young University, Provo UT, 2002, 195 pp.
[27] G. Barreiro, C.R.W. Guimarães, R. Bicca de Alencastro, Protein Eng. 16 (2003) 209–215.
[28] W.A. Sather, E.W. McCleskey, Annu. Rev. Physiol. 65 (2003) 133–159.
[29] D.J. Diestler, J. Chem. Phys. 117 (2002) 3411–3424.
[30] A.F. Bower, J.H. Weiner, J. Chem. Phys. 118 (2003) 11297–11306.
[31] S. Park, T. Khalili-Araghi, E. Tajkhorshid, K. Schulten, J. Chem. Phys. 119 (2003) 3559–3566.
[32] S.K. Bhatia, D. Nicholson, J. Chem. Phys. 119 (2003) 1719–1730.
[33] P.S. Crozier, R.L. Rowley, N.B. Holladay, D. Henderson, D.D. Busath, Phys. Rev. Lett. 86 (2001) 2467–2470.
[34] P.S. Crozier, D. Henderson, R.L. Rowley, D.D. Busath, Biophys. J. 81 (2001) 3077–3089.
[35] B. Zagrovic, C.D. Snow, M.R. Shirts, V.S. Pande, J. Mol. Biol. 323 (2002) 927–937.
[36] W.L. Jorgenson, J. Chandrasekar, J. Madura, R. Impley, M.L. Klein, J. Chem. Phys. 79 (1983) 926–935.

[37] B.R. Brooks, D.E. Bruccoleri, B.D. Olafson, D.J. States, S. Swaminathan, M. Karplus, J. Comput. Chem. 4 (1983) 187–217.
[38] J.P. Ryckaert, G. Ciccotti, J.P.C. Berendsen, J. Comput. Phys. 23 (1977) 327–341.
[39] E.W. McCleskey, J. Gen. Physiol. 113 (1999) 765–772.
[40] M.A. Wilson, A.T. Brunger, J. Mol. Biol. 301 (2000) 1237–1256.
[41] M. Overduin, T.S. Harvey, S. Bagby, K.I. Tong, P. Yau, M. Takeichi, M. Ikura, Science 267 (1995) 386–389.
[42] M.N.O. Herzberg, J. James, J. Mol. Biol. 203 (1988) 761–779.
[43] J. Kordel, N.J. Skelton, M. Akke, W.J. Chazin, J. Mol. Biol. 231 (1993) 711–734.